PHYSICAL REVIEW B VOLUME 60, NUMBER 24 15 DECEMBER 1999-II

Oxygen isoelectronic impurity in ZnS_xTe_{1-x}

M. J. Seong, H. Alawadhi, I. Miotkowski, and A. K. Ramdas
Department of Physics, Purdue University, West Lafayette, Indiana 47907

S. Miotkowska
Institute of Physics, Polish Academy of Sciences, AL. Lotnikow 32/46, 02-668 Warsaw, Poland

(Received 18 August 1999)

The binding energy of excitons bound to oxygen isoelectronic impurity in ZnS_xTe_{1-x}, shows a remarkable scaling with the difference between the electronegativity of oxygen and the concentration-weighted average of those of S and Te. The signatures of the free exciton, observed with wavelength modulated reflectivity, and those of shallow acceptor bound excitons, revealed in photoluminescence, show an unmistakable *redshift* with increasing x ($0 \leqslant x \leqslant 0.13$). In striking contrast, the excitons bound to the isoelectronic oxygen center in these alloys manifest a *blueshift* with increasing x. [S0163-1829(99)51148-X]

An isoelectronic impurity in a semiconductor often surprisingly binds an exciton, in spite of its isovalency with respect to the host atom it replaces. This occurs when there is a large electronegativity difference between them, resulting in a short range potential in which the exciton is trapped.[1] A striking example is oxygen in ZnTe,[2] which produces excitonic bound states in the otherwise forbidden energy gap, leading to a most remarkable photoluminescence (PL) spectrum as well as an absorption spectrum. The absorption and the emission spectra are ''mirror images'' with respect to a common no-phonon line (NPL). In contrast, an isoelectronic substituent differing slightly in its electronegativity from that of the host atom it replaces easily forms an alloy with the host, as in ZnS_xTe_{1-x}. In this context, it is clearly of interest to study an isoelectronic impurity in a system where the electronegativity of the host atom it replaces can be altered in a controlled fashion, e.g., oxygen in ZnS_xTe_{1-x}. In the spirit of virtual crystal approximation, the average anion electronegativity of ZnS_xTe_{1-x} can be viewed as a concentration-weighted average of those of S and Te. Since the electronegativity of oxygen differs more from that of Te than from that of S, it is natural to expect a decrease in the binding energy of excitons bound to oxygen as the sulfur concentration increases, as discussed and explored by Iseler and Strauss.[3] By combining the advantages of wavelength modulated reflectivity in discovering free excitonic signatures, and of PL in observing those of oxygen-bound excitons, we have investigated the problem quantitatively as a function of the sulfur concentration in ZnS_xTe_{1-x}. The spectra are recorded on the *same* set of specimens whose alloy compositions have been accurately determined with electron microprobe analysis. A *quantitative correlation* of the binding energy of excitons bound to oxygen centers with the *effective* anion electronegativity and the evolution of the alloy disorder broadening of the phonon replicas emerge unambiguously from the investigation reported in this paper.

Single crystals of ZnS_xTe_{1-x} were grown using a modified Bridgman technique. Oxygen doping was achieved with the addition of a small amount of ZnO powder to the source material inside a quartz ampoule. For the absorption measurement, both sides of the sample were polished to a surface roughness of ~ 0.5 μm. Cleaved as well as polished specimens were used for the PL studies. The actual sulfur composition of the samples was determined with a JOEL JSM-6400 scanning electron microscope using a LINK data analysis system for energy dispersive microanalysis. The free excitonic signature of the ternary alloy was discovered by recording wavelength modulated reflectivity spectra, using a SPEX (Model 1870) 0.5-m monochromator; a vibrating mirror inside the monochromator modulated at 85 Hz the wavelength of the light from a tungsten lamp source. The light reflected by the optical specimen, typically cooled down to 10 K in a Janis SuperTran cryostat, was detected with a silicon photodiode followed by a lock-in amplifier. The PL spectra were recorded with a SPEX (Model 14018) 0.85-m double grating monochromator. The samples were excited using the 4880-Å line from a Spectra-Physics Ar^+ laser. The sample temperature was controlled from 1.5 K to 10 K in a Janis 10-DT cryostat, and an RCA (type C31034A) photomultiplier was used as a detector. Absorption measurements were carried out using a Xe lamp as a white light source. The transmitted spectra were recorded with a SPEX (Model 1403) 0.85-m double grating monochromator, and an RCA (type C31034A) photomultiplier as a detector.

As a background for the discussion of the experimental results, it is useful to briefly recall the salient features of the isoelectronic oxygen impurity in ZnTe. The NPL in PL is accompanied by rich phonon replicas on the lower-energy side, representing the creation of LO, TO, LA, and TA phonons as well as combinations of them; in absorption, in contrast, they are ''mirrored'' on the high-energy side of the NPL. These phonon replicas are distinctly resolved at low temperatures. The temperature dependence of the NPL in the emission spectrum exhibits the $J=1$ and $J=2$ doublet resulting from the exchange interaction between a $j_h=\frac{3}{2}$ hole and a $j_e=\frac{1}{2}$, which is characteristic of an excitonic state for an isoelectronic trap in a zinc-blende semiconductor.[4,5] Transitions from the $J=1$ upper level of the doublet to the $J=0$ ground state (A-line) are electric dipole allowed while those from the $J=2$ lower level (B-line) are electric dipole forbidden. However, as the temperature is reduced below 5 K, the upper level is thermally depopulated and a new emis-

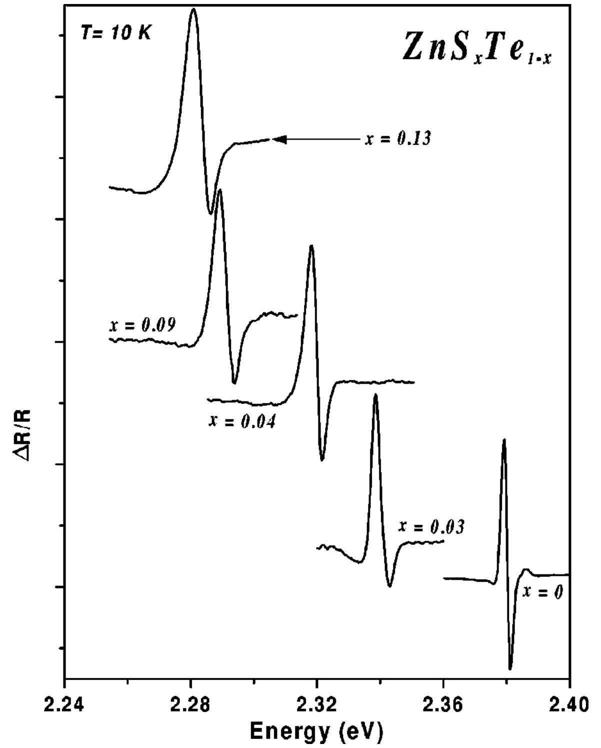

FIG. 1. Wavelength modulated reflectivity spectra displaying the free excitonic signatures in ZnS_xTe_{1-x} for $0 \leqslant x \leqslant 0.13$ at $T = 10$ K. The spectra are shifted vertically for clarity.

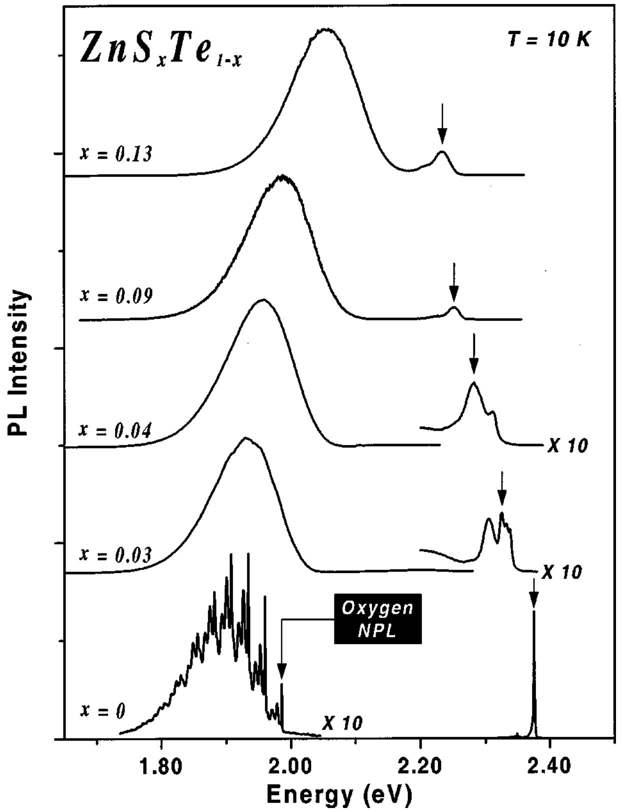

FIG. 2. Photoluminescence (PL) spectra of ZnS_xTe_{1-x} for $0 \leqslant x \leqslant 0.13$, showing the signature of the exciton bound to a shallow acceptor, identified with an arrow, and oxygen emission band. The spectra are shifted vertically for clarity.

sion line is observed originating from the $J = 2$ state. That the dipole-forbidden *B*-line is observed at all is partly due to phonon assisted mixing of the $J = 2$ and $J = 1$ states and partly due to a relaxation of the selection rules, presumably caused by residual strains around the oxygen center.[6]

The free exciton of ZnS_xTe_{1-x}, recorded as a derivative signature observed in wavelength modulated reflectivity, is displayed in Fig. 1 as a function of *x* in the range $0 \leqslant x \leqslant 0.13$. As can be seen, the energy of the free exciton, $E_g(x)$, decreases with increasing *x* in this range. In a recent investigation[7] it was observed that $E_g(x)$ in ZnS_xTe_{1-x}, as well as in $ZnSe_xTe_{1-x}$, indeed decreases before it eventually increases towards the value for ZnS and ZnSe, respectively. The signatures in wavelength modulated spectra show a distinct alloy broadening with *x*. The PL spectra of ZnS_xTe_{1-x} $(0 \leqslant x \leqslant 0.13)$ in Fig. 2 show features, identified with arrows, attributed to exciton bound to a shallow acceptor.[8] It is clear that the shallow acceptor bound excitonic feature tracks the position of the free exciton and confirms the decrease of $E_g(x)$ shown in Fig. 1. In contrast, the energy of the excitons bound to oxygen isoelectronic impurity shifts as a function of *x* in a direction *opposite* to that exhibited by the shallow acceptor bound exciton. For $x = 0$, the oxygen luminescence shows the very sharp NPL as well as the distinctive signatures associated with emission of the LO phonon and its overtones. The NPL and the LO phonon replicas in turn are accompanied by the emission of TA, LA, and TO phonons. It is remarkable that even with a small addition of S, the phonon replica signatures are obliterated. This is evidently a consequence of an alloy broadening of the NPL and its phonon replicas.

The remarkable evolution of the isoelectronic oxygen PL signature from the distinctive phonon structure for $x = 0$ to the structureless broad band for $x = 0.03$ is displayed in Fig. 3. With $x = 0.0025$, the NPL can still be observed, and the overtones of its LO phonon replica as well as acoustic phonon replicas are distinctly observed, although the NPL and all its phonon replicas are already broadened slightly and shifted to higher energies. For $x = 0.005$, the NPL and its LO phonon and acoustic phonon replicas are broadened more and blue-shifted further. At $x = 0.01$, the NPL and its phonon replicas are barely resolved, although their LO phonon replicas can still be resolved. At $x = 0.03$ all the phonon structures have disappeared, and the emission band coalesces into a single broad band. In the inset of Fig. 3, the absorption and the emission mirror images of the isoelectronic oxygen in $ZnS_{0.005}Te_{0.995}$ is shown as a typical example. In addition to the occurrence of the absorption and emission spectra of the oxygen center as mirror images of each other, the PL spectrum of $ZnS_{0.005}Te_{0.995}$ shows a small redshift as the temperature decreases from 10 K to 1.6 K. This results from the fact that the *B*-line, though electric dipole forbidden, dominates the *A*-line as a consequence of the thermal depopulation of the upper level at 1.6 K, from which the *A*-line originates.[5]

The overall vibronic structure of the isoelectronic impurities, as in the case of the oxygen center in ZnTe, has been explained on the basis of the Franck-Condon principle, which leads to a Poisson distribution for the intensities of the LO phonon replicas for both emission and absorption at low temperatures, $S^n e^{-S}/n!$, where *n* is the number of emitted

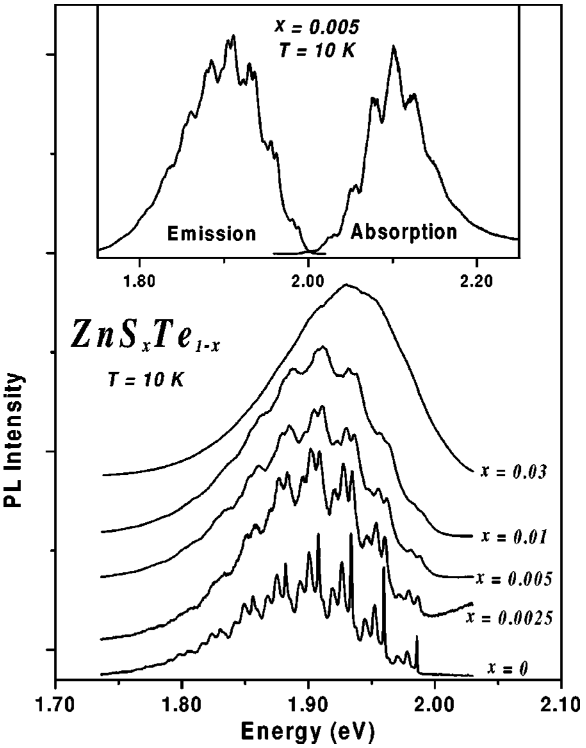

FIG. 3. PL spectra of oxygen emission band in $\mathrm{ZnS}_x\mathrm{Te}_{1-x}$ for $0 \leqslant x \leqslant 0.03$, showing the alloy broadening in detail. The spectra are shifted vertically for clarity. The occurrence of the emission and absorption spectra of the oxygen center in $\mathrm{ZnS}_{0.005}\mathrm{Te}_{0.995}$ as mirror images is underscored in the inset.

LO phonons and S the most probable number of phonons.[5,9,10] The peak of the broad feature, produced for $0.01 \leqslant x$ by the alloy broadened phonon replicas, shifts towards higher energy with increasing x while the energy of the excitons bound to shallow acceptors decreases. It is thus obvious that the binding energy of the exciton bound to the oxygen center *decreases with increasing* x. In order to make this deduction more quantitative, it is useful to estimate as accurately as possible the energy of NPL. Since the width and overall shape of the oxygen luminescence band does not change very much with x, the peak position of the broad spectrum for large x can be viewed as the maximum of the superposition of all the phonon features corresponding to those observed for $x=0$, but alloy broadened. On the basis of this model, this distinctive feature of the oxygen luminescence band can be fitted using a "continuous" analog of the Poisson distribution.[11] To the extent the curve can be fitted with the same distribution, we can deduce the NPL energy for large x, where the distinct NPL signature is no longer observed, by assuming that the difference in energy between this broad fitted peak and the NPL can be reasonably expected to be the same (87 meV) for small values of x, e.g., in the range $0 \leqslant x \leqslant 0.13$ studied in the present work. Thus we have implicitly assumed the same values of S and $\hbar\omega_{LO}$ for $0 \leqslant x \leqslant 0.13$; the change in the ZnTe-like LO phonon frequency is available directly from the Raman spectra we have studied and found to be about 0.1 meV, justifying the use of the same ZnTe LO phonon energy in the analysis. Viewed in this manner, the energy of the NPL can be reliably deduced by adding to the peak position of each fitted distribution, 87 meV, calculated for ZnTe, where the NPL is directly observed. The energies of the NPL thus extracted and the band gap measured with wavelength modulated reflectivity as a function of x are displayed in Fig. 4(a). The NPL energy position of the oxygen center in $\mathrm{ZnS}_x\mathrm{Te}_{1-x}$ increases as the band gap decreases, the rate at which the binding energy decreases being larger than that of the band gap energy decrease. The binding energy of the exciton bound to the oxygen center shown in Fig. 4(b) is seen to decrease linearly with increasing x. This linear behavior is consistent with a model, which assumes the virtual crystal approximation for the anion electronegativity of the alloy.

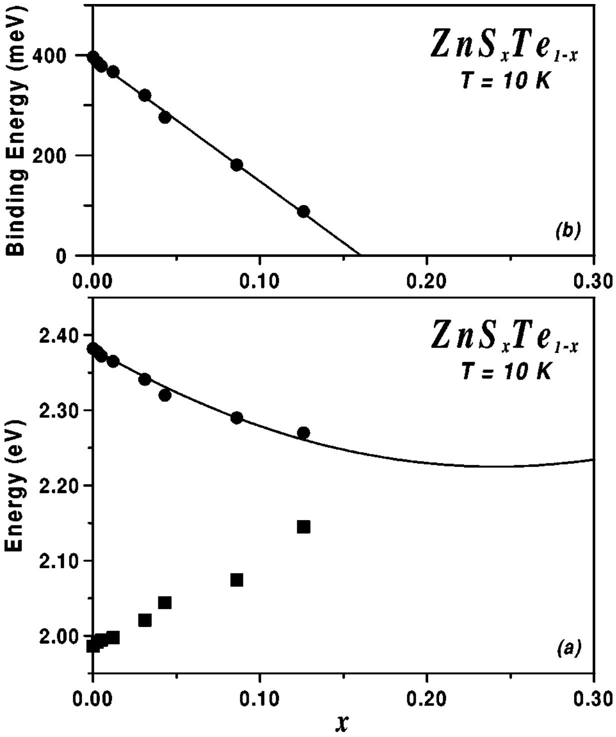

FIG. 4. (a) The NPL energy of the exciton bound to oxygen center (solid squares) and the energy of the free exciton measured with wavelength modulated reflectivity (full circles) as a function of x. The solid line is a quadratic fit for the band gap variation of $\mathrm{ZnS}_x\mathrm{Te}_{1-x}$. (b) The binding energy of the exciton bound to oxygen center as a function of x is displayed along with a linear fit (solid line).

In the present study, the combined advantages of different types of spectroscopies have led to a microscopic insight into a physically important parameter, *viz.* the "effective" *anion electronegativity* in $\mathrm{ZnS}_x\mathrm{Te}_{1-x}$ as a function of x. The convergence of the free exciton signature with its redshift and the oxygen luminescence band characterized by its blueshift, observed with increasing x in the range $0 \leqslant x \leqslant 0.13$, enables the decrease in binding energy of the exciton bound to the oxygen center in $\mathrm{ZnS}_x\mathrm{Te}_{1-x}$ to be exposed in an unambiguous manner. A significant outcome of this study is that the binding energy of the exciton bound to the oxygen center scales with the difference between the electronegativity of oxygen and the "effective" electronegativity of the anion, "$\mathrm{S}_x\mathrm{Te}_{1-x}$", in $\mathrm{ZnS}_x\mathrm{Te}_{1-x}$ considered in the spirit of the *virtual crystal approximation for the anion electronegativity* of the alloy. It is demonstrated that the binding energy of excitons bound to oxygen in $\mathrm{ZnS}_x\mathrm{Te}_{1-x}$ extrapolates to zero for $x=0.16$. Indeed, it would be of interest to explore the nature of the oxygen isoelectronic impurity for x larger than 0.16.

The authors acknowledge support from National Science Foundation Grant No. DMR 98-00858 and Grant No. 94-00415 (Materials Research Science and Engineering Center).

---

[1] J. J. Hopfield, D. G. Thomas, and R. T. Lynch, Phys. Rev. Lett. **17**, 312 (1966).

[2] R. E. Dietz, D. G. Thomas, and J. J. Hopfield, Phys. Rev. Lett. **8**, 391 (1962).

[3] G. W. Iseler and A. J. Strauss, J. Lumin **3**, 1 (1970).

[4] J. L. Merz, Phys. Rev. **176**, 961 (1968).

[5] M. J. Seong, I. Miotkowski, and A. K. Ramdas, Phys. Rev. B **58**, 7734 (1998).

[6] W. Czaja, *Isoelectronic Impurities in Semiconductors*, in *Festkörprobleme XI*, edited by O. Madelung (Pergamon, Oxford, 1971) pp. 65–85.

[7] M. J. Seong, H. Alawadhi, I. Miotkowski, A. K. Ramdas, and S. Miotkowska, Solid State Commun. **112**, 329 (1999).

[8] H. Venghaus and P. J. Dean, Phys. Rev. B **21**, 1596 (1980).

[9] V. Slusarenko, Y. Burki, W. Czaja, and H. Berger, Phys. Status Solidi B **161**, 897 (1990).

[10] A. Testa, W. Czaja, A. Quattropani, and P. Schwendimann, J. Phys. C **20**, 1253 (1987).

[11] $S^{[(E_0-E)/\hbar\omega_{LO}]}e^{-S}/\Gamma[(E_0-E)/(\hbar\omega_{LO})+1]$, where $\Gamma(n+1)=n!$ is the gamma function and $\hbar\omega_{LO}$ is the energy of the LO phonon of ZnTe. This function is derived from the Poisson distribution, $S^n e^{-S}/n!$, by substituting the discrete variable n for a continuous one, $[(E_0-E)/\hbar\omega_{LO}]+1$, where E is the energy of an emitted photon.